52nd AIAA/ASME/ASCE/AHS/ASC Structures, Structural Dynamics and Materials Conference
 19th
4 - 7 April 2011, Denver, Colorado

AIAA 2011-2065

Reduced Order Modeling for Nonlinear Vibration Analysis of Mistuned Multi-Stage Bladed Disks with a Cracked Blade

Kiran D'Souza, Akira Saito, and Bogdan I. Epureanu*

Department of Mechanical Engineering

University of Michigan, Ann Arbor, MI 48109-2125

In this paper, a novel modeling methodology for the nonlinear vibration analysis of multi-stage bladed disk systems with small blade-to-blade mistuning and a cracked blade is proposed. The modeling strategy is based on an efficient stage-wise reduced order modeling method based on cyclic-symmetry analysis and component mode synthesis. Reduced order models are constructed for individual stages and assembled by projecting the motion of the interface of the neighboring stages onto a set of harmonic shape functions. The analysis procedure allows the stages to have different numbers of blades and mismatched computational grids on the interfaces of the neighboring stages. Furthermore, the modeling framework is independent of the modeling method for each stage, which enables the use of various existing modeling methods of single stages. Moreover, nonlinearity can also be included in the multi-stage computations, as long as the nonlinearity can be modeled for a single stage. To demonstrate the capability of the modeling procedure, the nonlinear effect of crack opening and closing is considered, in conjunction with the effects of small mistuning. The accuracy and efficiency of the proposed methods are discussed.

Nomenclature

b	DOFs along the inter-stage boundary of a sector of stage 1
$\mathbf{F}_{n\times m}$	Fourier matrix of size $n \times m$
$\mathbf{f}$	nonlinear forces due to intermittent contact at the crack surfaces
$\mathbf{I}_n$	identity matrix of size $n \times n$
i	set of internal (not along the inter-stage boundary) DOFs
$\mathbf{K}$	stiffness matrix of a single sector of a stage
$\mathbf{M}$	mass matrix of a single sector of a stage
M_r	number of DOFs in each radial line segment for stage 2
N	number of sectors in stage 1
N_b	number of DOFs along the inter-stage boundary for a sector in stage 1
$N_{\tilde{b}}$	number of DOFs along the inter-stage boundary for stage 2
N_r	number of DOFs in each radial line segment for stage 1
N_s	number of DOFs in a sector of stage 1
$\mathbf{p}_h$	set of modal coordinates associated with the fixed-interface normal modes of stage 1
$\mathbf{q}(t)$	set of modal coordinates associated with the free-interface normal modes of stage 2
$\mathbf{R}_b^h$	forces applied at the inter-stage boundary DOFs that cause a unit displacement at each DOF while keeping the rest of the DOFs along the boundary fixed
$\mathbf{u}_{c,s}^h$	vector of Fourier coefficients, superscript h denotes the harmonic number, and subscript c or s denote cosine or sine component
$\mathbf{u}_b^h$	vector of Fourier coefficients corresponding to the inter-stage boundary, superscript h denotes the harmonic number
$\mathbf{u}_i^h$	vector of Fourier coefficients corresponding to the internal DOFs, superscript h denotes

*Corresponding author: B. I. Epureanu, epureanu@umich.edu

	the harmonic number
W	number of radial line segments per sector for stage 2
$\mathbf{x}(t)$	nodal displacement of all nodes on all sectors of stage 1
$\mathbf{x}_b(t)$	nodal displacement along the inter-stage boundary of stage 1
$\mathbf{y}(t)$	nodal displacement of all nodes of stage 2
$\mathbf{y}_b(t)$	nodal displacement along the inter-stage boundary of stage 2
$\mathbf{y}_i(t)$	nodal displacement of all internal DOFs of stage 2
Z	number of radial line segments per sector for stage 1
α	boundary of a sector considered to be moving independently
β	boundary of a sector considered to be dependent on the movement of the independent boundary due to the constraints
Δ	DOFs in the blade portion of a sector
Γ	DOFs in the disk portion of a sector
κ_j	collection of stiffness matrices of disconnected sectors
μ_j	collection of mass matrices of disconnected sectors
ϕ_h	inter-blade phase angle
$\mathbf{\Phi}_i^h$	fixed-interface normal modes for harmonic number h
$\tilde{\mathbf{\Phi}}_i$	modified free-interface normal modes
φ_h	fixed inter-face normal mode
$\mathbf{\Psi}_i^h$	constraint modes for harmonic number h
ω_k	natural frequency corresponding to the k^{th} free-interface normal mode
$\mathcal{L}$	Lagrangian of a stage
$\mathcal{T}$	kinetic energy of a stage
$\mathcal{U}$	potential energy of a stage

I. Introduction

With the concurrent advancement of computer hardware and software with sophisticated physical and mathematical methodologies represented by finite element method, model-based vibration analysis has been extensively applied to the dynamic analysis of turbomachinery rotors. Most turbine engine rotors consist of multiple stages of bladed disks. Vibration modeling of rotors is a classic problem, yet it has been an active research area for structural dynamicists both in industry and academia. In this paper, a novel reduced order modeling method is proposed for the vibration problems of multi-stage bladed disk assemblies, which possess a cracked blade on one of the stages, and is subject to blade-to-blade small mistuning. The methodology allows the use of an efficient cyclic-symmetry based reduced order modeling method for mistuned but non-cracked stages. The modeling framework is developed by generalizing the modeling procedure proposed by Song *et al.*[1] and is described in the *Mathematical Formulation* section.

This paper is organized as follows. First, a brief overview of multi-stage turbomachinery analysis is provided. Then, a mathematical description of the proposed modeling approach is described. Next, the proposed methodology is validated by using a numerical example of an industrial multi-stage bladed disk system. In particular, nonlinear forced response calculations are performed, and the applicability of the proposed method to the vibration problem of multi-stage bladed disks is demonstrated. Finally, conclusions of the work are given.

II. Background

An extensive literature survey of linear and nonlinear vibration modeling of mistuned bladed disk systems is given by Castanier and Pierre.[2] Bladh *et al.*[3] investigated the effects of multi-stage coupling on the dynamics of bladed disks with blade mistuning. It was pointed out that the mistuning due to inter-stage coupling is inherent in multi-stage systems. Furthermore, it was reported that the inter-stage coupling may be significant and cannot be neglected when the frequency ranges of interest pass *veering regions*, where the motion of the disk is dominant. A novel reduced order modeling technique for multi-stage bladed disk systems was proposed by Song *et al.*,[4] which enables the use of stage-wise reduced order models (ROMs) by cyclic-symmetry. The method was then incorporated[5] with an efficient mistuning modeling method called

component mode mistuning (CMM).[6] It was successfully applied to the modal parameter identification of multi-stage bladed disks,[7] and also to mistuning identification and structural health monitoring.[1] Laxalde *et al.*[8] also proposed a method to deal with multi-stage bladed disk systems with a similar concept as that proposed by Song *et al.*,[1] and successfully applied their method to modal analysis and forced response calculations for industrial bladed disks.[9] However, in that work each stage was assumed to be tuned. Sternchüs *et al.*[10] extended the method proposed by Laxalde *et al.*,[8,9] by representing the inter-sector elements as super-elements, and by using inter-stage ring elements. The methodology presented in this paper is a generalization of the method proposed by Song *et al.*,[1] which applies the inter-stage compatibility by Fourier coefficients, and handles the mistuning with CMM.[6]

Sinha[11] also developed a lumped parameter model of mistuned multi-stage models where inter-stage coupling is handled by discrete springs, and conducted Monte Carlo simulations on these models. Although the model was shown to be able to simulate the overall dynamics of the multi-stage rotors, its applicability to industrial models with realistic geometry was not discussed.

In addition to the modeling of blades, there have also been efforts to accurately capture the coupling effects between the torsional vibration of shafts and blades. For example, Chatelet *et al.*[12] investigated the complicated dynamics of rotors and shafts by assuming that all the rotors and shafts are axisymmetric and by applying cyclic-symmetry analysis. Turhan and Bulut[13] considered the coupling between shaft torsion and blade bending vibrations by using a qualitative model of multi-stage bladed disks, where the disks are modeled as rigid and the blades are modeled as Euler-Bernoulli beams. Their eigenanalysis (of the analytical model) indicated that there are two types of modes: the coupled modes where shaft torsion and blade bending are coupled, and the rigid shaft modes where the dominant motion is a rigid-body motion of the disk and blades. They also reported that the coupled shaft torsion and blade bending modes are subject to eigenvalue loci veering.

Rzadkowski and Sokolwski,[14] and Rzadkowski and Drewczynski[15] examined the free response of an eight bladed disk assembly connected by a flexible shaft. For that specific model, they reported that the bladed disk modes of nodal diameters zero, one and two are affected by the shaft flexibility, and multi-stage effects are visible. However, they assumed that the bladed disks are all tuned and have the same number of blades. That is a significant drawback which means that the entire multi-stage bladed disk system has to be cyclically symmetric.

Seguì and Casanova[16] also developed a reduced order modeling method for a (single stage) mistuned bladed disk mounted on a shaft. The method utilizes the Craig-Bampton component mode synthesis (CMS) method[17] where the blades, the disk, and the shaft are considered to be separate substructures. As was also reported by other researchers, their work suggested that the stage-wise modal analysis is not enough for accurately predicting the global dynamic response of rotating turbomachines. Later, Boulton and Casanova[18] extended the modeling approach of Seguì and Casanova[16] to the dynamical modeling of a two-stage, mistuned, industrial gas turbine model, and showed that the interaction between the bladed disk and shaft contributes to the variations in the modes predicted from the stage-wise modal analysis.

All the references cited above deal with *linear* vibration problems. Nonlinearity comes from various sources in the dynamics of turbomachinery rotors. To date, only a few attempts have been made to deal with a multi-stage bladed disk assembly with nonlinearities. Laxalde and Thouverez[19] investigated the modeling of friction-ring dampers, which cause strong nonlinearity due to friction between the rotors and the dampers. The nonlinear forced response analysis was performed based on a multi-harmonic hybrid-frequency time domain method with an augmented Lagrangian approach.[20] They showed the applicability of the reduced order modeling of the multi-stage bladed disks based on cyclic-symmetry, and the multi-harmonic hybrid-frequency time domain method.

There have been only a few papers published to date regarding the issue of vibration problems of bladed disks with cracked blades. Saito *et al.*[21] investigated the effects of a cracked blade on the forced response vibration of a single stage mistuned bladed disk. They revealed that there can be a cracked-blade-localized vibration response for some families of modes. Kharyton *et al.*[22] also investigated the effects of a cracked blade on the vibration response of a bladed disk without blade-to-blade mistuning.

III. Mathematical Formulation

In this section, the proposed reduced order modeling method for multi-stage bladed disk assemblies is described. When modeling the multi-stage bladed disk assemblies, the challenge is that the entire multi-stage

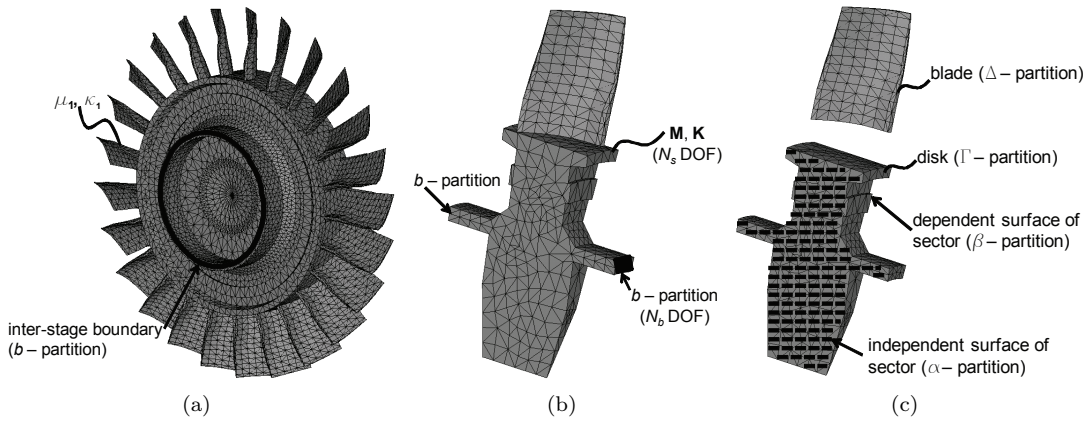

Figure 1. (a) Cyclic stage with N sectors, (b) single sector of the cyclic stage, (c) blade and disk partitions of the sector model.

assembly does not possess cyclic-symmetry because the stages do not necessarily have the same number of blades. Therefore, any reduced order modeling method based on cyclic-symmetry suffers from this issue. Furthermore, efficient modeling of mistuning is crucial for statistical analyses such as Monte-Carlo simulations for many mistuning patterns. The proposed method addresses these challenges.

Recently, efficient mistuning modeling methods for a single stage bladed disk have been reported. For example the CMM approach proposed by Lim *et al.*[6] was shown to be effective and accurate for single stage bladed disks. Song *et al.*[1] successfully applied CMM for the modeling of multi-stage bladed disks. The methodology is capable of modeling the mistuned bladed disks based on a stage-wise cyclic CMS method, and the application of compatibility conditions at the inter-stage boundaries using Fourier basis functions. In this paper, this modeling framework is further generalized for the cases where the system consists of a mixture of stages that in the absense of small blade-to-blade mistuning can be modeled by cyclic-symmetry, and those that cannot be modeled by cyclic-symmetry. Herein, a bladed disk that can be modeled via cyclic-symmetry is referred to as a *cyclic stage*. Strictly speaking, if there is blade-to-blade mistuning, no stage possesses cyclic-symmetry. However, the small mistuning can be added to a stage modeled by cyclic-symmetry by using CMM.[6] Furthermore, the stage that cannot be modeled via cyclic-symmetry is referred to as a *non-cyclic stage*. These stages cannot be modeled via cyclic-symmetry for various reasons, e.g., the presence of large geometric variations, symmetry-breaking components, or a cracked blade. In this paper, the disk with a cracked blade is treated as a non-cyclic stage.

The modeling framework is designed such that it is capable of modeling each stage separately, and it can handle any small mistuning pattern efficiently. First, the model reduction method is formulated for cyclic stages (with distinct number of blades). Then it is formulated for non-cyclic stages. Finally, the assembly of the stage-wise ROMs is discussed.

A. Reduced Order Modeling of Cyclic Stages

1. Modeling of Cyclic Stages

Let us assume that stage 1 of a multi-stage system is cyclic and consists of N identical sectors that are disconnected. Fig. 1(a) shows a cyclic stage where N is equal to 25, and Fig. 1(b) shows one of the N sectors that make up the stage. Let $\mathbf{x}(t)$ denote the nodal displacement of all nodes on all sectors. Their kinetic and potential energies can be written as $\mathcal{T} = (1/2)\dot{\mathbf{x}}^{\mathrm{T}}\boldsymbol{\mu}_1\dot{\mathbf{x}}$ and $\mathcal{U} = (1/2)\mathbf{x}^{\mathrm{T}}\boldsymbol{\kappa}_1\mathbf{x}$, where $\boldsymbol{\mu}_1$ and $\boldsymbol{\kappa}_1$ represent the collections of matrices of the disconnected sectors, i.e.,

$$\begin{aligned} \boldsymbol{\mu}_1 &= \mathbf{I}_N \otimes \mathbf{M}, \\ \boldsymbol{\kappa}_1 &= \mathbf{I}_N \otimes \mathbf{K}, \end{aligned} \tag{1}$$

where $\mathbf{M}$ and $\mathbf{K}$ denote the mass and the stiffness matrices of a sector, $\mathbf{I}_N$ is an identity matrix of size $N \times N$, and $\otimes$ denotes a Kronecker product. Partitioning the displacement vector such that they are ordered

based on the order of the sectors, i.e., $\mathbf{x} = [\mathbf{x}_1^{\mathrm{T}}, \dots \mathbf{x}_N^{\mathrm{T}}]^{\mathrm{T}}$, it is known[1,6] that the displacements of the n^{th} sector can be exactly described by the following Fourier series

$$\mathbf{x}_n = \frac{1}{\sqrt{N}}\mathbf{u}^0 + \sqrt{\frac{2}{N}}\sum_{h=1}^{\tilde{N}-1}\left(\mathbf{u}_c^h \cos(n-1)\phi_h + \mathbf{u}_s^h \sin(n-1)\phi_h\right) + \frac{1}{\sqrt{N}}(-1)^{n-1}\mathbf{u}^{\tilde{N}}, \tag{2}$$

where $\phi_h = 2\pi h/N$, $n = 1, \dots, N$ and $\tilde{N} = N/2$ if N is even, or $\tilde{N} = (N-1)/2$ if N is odd. $\mathbf{u}$ denotes a vector of Fourier coefficients, subscripts c and s denote cosine and sine components respectively, and superscripts denote the harmonic number. Also, the last term in Eq. (2) does not exist when N is odd. The transformation from the Fourier coefficients $\tilde{\mathbf{u}}$, to physical coordinates $\mathbf{x}$ can be written as a linear map

$$\mathbf{x}(t) = (\mathbf{F}_{N,N} \otimes \mathbf{I}_{N_s})\tilde{\mathbf{u}}(t), \tag{3}$$

where

$$\tilde{\mathbf{u}} = [(\mathbf{u}^0)^{\mathrm{T}}, (\mathbf{u}_c^h)^{\mathrm{T}}, (\mathbf{u}_s^h)^{\mathrm{T}}, \dots, (\mathbf{u}^{\tilde{N}})^{\mathrm{T}}]^T, \tag{4}$$

and N_s is the number of degrees of freedom (DOFs) in a sector. For the sake of brevity, let us now partition the nodal displacement vector for a sector, and corresponding Fourier coefficients based on the physical partitions of the finite element model (FEM). Namely, the Fourier coefficients are partitioned as $\mathbf{u}^h = [(\mathbf{u}_\Delta^h)^{\mathrm{T}}, (\mathbf{u}_\Gamma^h)^{\mathrm{T}}, (\mathbf{u}_b^h)^{\mathrm{T}}]^T$, where Δ, Γ and b correspond to the DOF sets for the nodes of the blade part, disk part, and the inter-stage boundary as shown in Fig. 1(c). Substituting Eq. (4) into the kinetic and potential energies, the Lagrangian of this stage can be expressed with the Fourier coefficients as

$$\begin{aligned}\mathcal{L} &= \frac{1}{2}\dot{\mathbf{x}}^{\mathrm{T}}\boldsymbol{\mu}_1\dot{\mathbf{x}} - \frac{1}{2}\mathbf{x}^{\mathrm{T}}\boldsymbol{\kappa}_1\mathbf{x} \\ &= \frac{1}{2}\dot{\tilde{\mathbf{u}}}^{\mathrm{T}}(\mathbf{F}_{N,N} \otimes \mathbf{I}_{N_s})^{\mathrm{T}}(\mathbf{I}_N \otimes \mathbf{M})(\mathbf{F}_{N,N} \otimes \mathbf{I}_{N_s})\dot{\tilde{\mathbf{u}}} - \frac{1}{2}\tilde{\mathbf{u}}^{\mathrm{T}}(\mathbf{F}_{N,N} \otimes \mathbf{I}_{N_s})^{\mathrm{T}}(\mathbf{I}_N \otimes \mathbf{K})(\mathbf{F}_{N,N} \otimes \mathbf{I}_{N_s})\tilde{\mathbf{u}}.\end{aligned}$$

Hamilton's principle requires the action integral be stationary, i.e.,

$$\delta \int_{t_1}^{t_2} \mathcal{L}(\tilde{\mathbf{u}}, \dot{\tilde{\mathbf{u}}})\mathrm{d}t = 0. \tag{5}$$

Without any constraint between the (identical) sectors, this yields the following set of equations of motion

$$\begin{gathered}\mathbf{M}\ddot{\mathbf{u}}^0 + \mathbf{K}\mathbf{u}^0 = \mathbf{0}, \\ \begin{pmatrix}\mathbf{M} & \mathbf{0} \\ \mathbf{0} & \mathbf{M}\end{pmatrix}\begin{bmatrix}\ddot{\mathbf{u}}_c^h \\ \ddot{\mathbf{u}}_s^h\end{bmatrix} + \begin{pmatrix}\mathbf{K} & \mathbf{0} \\ \mathbf{0} & \mathbf{K}\end{pmatrix}\begin{bmatrix}\mathbf{u}_c^h \\ \mathbf{u}_s^h\end{bmatrix} = \begin{bmatrix}\mathbf{0} \\ \mathbf{0}\end{bmatrix}, \quad \text{for} \quad h = 1, \dots, \tilde{N}-1, \\ \mathbf{M}\ddot{\mathbf{u}}^{\tilde{N}} + \mathbf{K}\mathbf{u}^{\tilde{N}} = \mathbf{0}.\end{gathered}$$

At this point, all the sectors are assumed to be disconnected. However, the symmetry in the circumferential direction implies that the nodal displacement field of one side of a sector is dependent on that of the other side of the sector. Furthermore, the constraints are dependent on the harmonic number. Namely, the equations of motion are derived by the extremization of the action integral in Eq. (5) subject to the constraints

$$\begin{aligned}\mathbf{u}_{c,\beta}^h &= \mathbf{u}_{c,\alpha}^h \cos\phi_h + \mathbf{u}_{s,\alpha}^h \sin\phi_h, \\ \mathbf{u}_{s,\beta}^h &= -\mathbf{u}_{c,\alpha}^h \sin\phi_h + \mathbf{u}_{s,\alpha}^h \cos\phi_h,\end{aligned} \tag{6}$$

where α represents the boundary considered to be independently moving (on one side of the boundary), β represents the boundary considered to be dependent on the movement of the α boundary (due to the constraints). After the application of Eq. (6) to Eq. (5), the equations of motion of the h^{th} harmonic number can be written in a partitioned format as

$$\left(\begin{array}{cc|c} \mathbf{M}_{i,0}^h & \mathbf{M}_{i,1}^h & \mathbf{M}_{ib}^h \\ (\mathbf{M}_{i,1}^h)^{\mathrm{T}} & \mathbf{M}_{i,0}^h & \\ \hline (\mathbf{M}_{ib}^h)^{\mathrm{T}} & & \mathbf{M}_b^h \end{array}\right)\begin{bmatrix}\ddot{\mathbf{u}}_{c,i}^h \\ \ddot{\mathbf{u}}_{s,i}^h \\ \ddot{\mathbf{u}}_b^h\end{bmatrix} + \left(\begin{array}{cc|c} \mathbf{K}_{i,0}^h & \mathbf{K}_{i,1}^h & \mathbf{K}_{ib}^h \\ (\mathbf{K}_{i,1}^h)^{\mathrm{T}} & \mathbf{K}_{i,0}^h & \\ \hline (\mathbf{K}_{ib}^h)^{\mathrm{T}} & & \mathbf{K}_b^h \end{array}\right)\begin{bmatrix}\mathbf{u}_{c,i}^h \\ \mathbf{u}_{s,i}^h \\ \mathbf{u}_b^h\end{bmatrix} = \mathbf{0}, \tag{7}$$

where

$$\mathbf{M}^h_{i,0} = \begin{pmatrix} \mathbf{M}_{\alpha\alpha} + \cos\phi_h(\mathbf{M}_{\beta\alpha} + \mathbf{M}_{\alpha\beta}) + \mathbf{M}_{\beta\beta} & \mathbf{M}_{\alpha\Delta} + \cos\phi_h\mathbf{M}_{\beta\Delta} \\ \mathbf{M}_{\Delta\alpha} + \cos\phi_h\mathbf{M}_{\Delta\beta} & \mathbf{M}_{\Delta\Delta} \end{pmatrix},$$

$$\mathbf{M}^h_{i,1} = \begin{pmatrix} (\mathbf{M}_{\alpha\beta} - \mathbf{M}_{\beta\alpha})\sin\phi_h & \sin\phi_h\mathbf{M}_{\beta b} \\ \sin\phi_h\mathbf{M}_{\Delta\beta} & \mathbf{0} \end{pmatrix},$$

$$\mathbf{M}^h_{ib} = \begin{pmatrix} \mathbf{M}_{\alpha b} + \cos\phi_h\mathbf{M}_{\beta b} & -\sin\phi_h\mathbf{M}_{\beta b} \\ \mathbf{M}_{\Delta b} & \mathbf{0} \\ \sin\phi_h\mathbf{M}_{\beta b} & \mathbf{M}_{\alpha b} + \cos\phi_h\mathbf{M}_{\beta b} \\ \mathbf{0} & \mathbf{M}_{\Delta b} \end{pmatrix},$$

$$\mathbf{M}^h_b = \begin{pmatrix} \mathbf{M}_{bb} & \mathbf{0} \\ \mathbf{0} & \mathbf{M}_{bb} \end{pmatrix},$$

and i denotes the set of internal DOF defined as $i \triangleq \{\alpha, \Delta, \Gamma\}$, and b denotes the set of DOF on the inter-stage boundary. The structure of the stiffness matrix is omitted here for the sake of brevity because it is the same as the one for the mass matrix.

2. *Reduced Order Modeling of Cyclic Stages by the Craig-Bampton Method*

For the reduction of the cyclic stages, the reduction method proposed by Song *et al.*[4] is employed. That method is based on the cyclic Craig-Bampton method developed by Bladh *et al.*[23] Namely, the displacement field of the entire stage $\mathbf{x}(t)$ is assumed to be represented as a linear combination of fixed-interface normal modes and constraint modes. The model reduction method with these types of modes is usually referred to as the Craig-Bampton method.[17] The fixed-interface normal modes are a truncated set of normal modes of the entire stage with all DOFs on the inter-stage boundary being fixed. A constraint mode for a stage is computed as the static deformation shape of the entire stage due to a unit displacement applied to one of its DOF on the inter-stage boundary (while all the other DOFs on the inter-stage boundary are fixed). A complete set of constraint modes is obtained by repeating such computation for all DOFs on the inter-stage boundary. One disadvantage of this method is that the computation of these constraint modes becomes prohibitively expensive as the model size grows. However, by the application of cyclic-symmetry, these modes can be efficiently computed by solving eigenvalue problems and static problems of a sector and a duplicated sector alone, with appropriate inter-sector boundary conditions. Recalling that the set of DOFs for the inter-stage boundary are denoted by a subscript b, and that all the other DOFs are denoted by a subscript i, the Fourier coefficients can be well approximated by the following coordinate transformation

$$\begin{bmatrix} \mathbf{u}^h_b \\ \mathbf{u}^h_i \end{bmatrix} \simeq \begin{pmatrix} \mathbf{I}_{N_b} & \mathbf{0} \\ \mathbf{\Psi}^h_i & \mathbf{\Phi}^h_i \end{pmatrix} \begin{bmatrix} \mathbf{u}^h_b \\ \mathbf{p}^h \end{bmatrix}, \quad \text{for} \quad h = 0, \ldots, \tilde{N}, \tag{8}$$

where N_b is the number of DOFs on the inter-stage boundary (the b-partition), the matrices $[\mathbf{I}_{N_b}, (\mathbf{\Psi}^h_i)^{\mathrm{T}}]^{\mathrm{T}}$ and $[\mathbf{0}, (\mathbf{\Phi}^h_i)^{\mathrm{T}}]^{\mathrm{T}}$ are called the constraint modes and the fixed-interface normal modes for harmonic number h, and $\mathbf{p}^h$ is the set of modal coordinates associated with the fixed-interface normal modes.

Assuming harmonic motion and substituting $\mathbf{u}(t) = \boldsymbol{\varphi} e^{\omega t}$ into Eq. (7), then the k^{th} fixed-interface normal mode for harmonic number h can be computed by solving the following eigenvalue problem

$$\begin{pmatrix} \mathbf{K}^h_{i,0} & \mathbf{K}^h_{i,1} \\ (\mathbf{K}^h_{i,1})^{\mathrm{T}} & \mathbf{K}^h_{i,0} \end{pmatrix} \begin{bmatrix} (\boldsymbol{\varphi}^h_{c,i}) \\ (\boldsymbol{\varphi}^h_{s,i}) \end{bmatrix}_k = \lambda_k \begin{pmatrix} \mathbf{M}^h_{i,0} & \mathbf{M}^h_{i,1} \\ (\mathbf{M}^h_{i,1})^{\mathrm{T}} & \mathbf{M}^h_{i,0} \end{pmatrix} \begin{bmatrix} (\boldsymbol{\varphi}^h_{c,i}) \\ (\boldsymbol{\varphi}^h_{s,i}) \end{bmatrix}_k, \quad \text{for} \quad k = 1, \ldots, m^h_1, \tag{9}$$

where $\lambda_k = \omega^2_k$, and m^h_1 denotes the number of free-interface normal modes to be kept for stage 1.

In contrast, the i-partition of the constraint modes can be computed by solving the following static problem for $\mathbf{\Psi}^h_{c,i}$ and $\mathbf{\Psi}^h_{s,i}$

$$\left(\begin{array}{cc|c} \mathbf{K}^h_{i,0} & \mathbf{K}^h_{i,1} & \mathbf{K}^h_{ib} \\ (\mathbf{K}^h_{i,1})^{\mathrm{T}} & \mathbf{K}^h_{i,0} & \\ \hline (\mathbf{K}^h_{ib})^{\mathrm{T}} & & \mathbf{K}^h_b \end{array}\right) \begin{pmatrix} \mathbf{\Psi}^h_{c,i} \\ \mathbf{\Psi}^h_{s,i} \\ \mathbf{I}_{N_b} \end{pmatrix} = \begin{pmatrix} \mathbf{0} \\ \mathbf{0} \\ \mathbf{R}^h_b \end{pmatrix}, \tag{10}$$

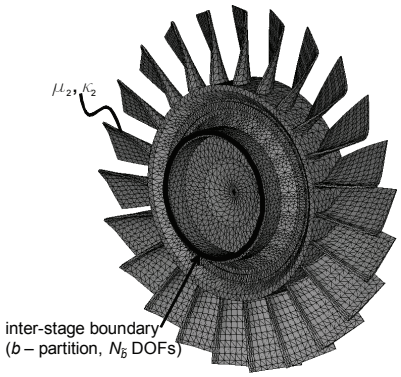

Figure 2. Non-cyclic stage with M sectors.

where $\mathbf{R}_b^h$ represents the forces applied to the inter-stage boundary, which cause a unit displacement at one DOF while keeping the rest of the DOFs along the boundary fixed, and N_b is the number of DOFs along the inter-stage boundary for the sector. Defining $\tilde{\mathbf{p}} \triangleq [(\mathbf{u}^0)^{\mathrm{T}}, (\mathbf{p}^0)^{\mathrm{T}}, \ldots, (\mathbf{u}^{\tilde{N}})^{\mathrm{T}}, (\mathbf{p}^{\tilde{N}})^{\mathrm{T}}]^{\mathrm{T}}$, the linear transformation between the Fourier coefficients for all harmonic numbers $\tilde{\mathbf{u}}(t)$ and the generalized coordinates $\tilde{\mathbf{p}}(t)$ can be written as

$$\tilde{\mathbf{u}}(t) \simeq \boldsymbol{\Phi}_{\mathcal{CB}}\ \tilde{\mathbf{p}}(t), \tag{11}$$

where

$$\boldsymbol{\Phi}_{\mathcal{CB}} = \underset{h=0,\ldots,\tilde{N}}{\mathrm{bdiag}} \begin{pmatrix} \mathbf{I}_{N_b} & \mathbf{0} \\ \boldsymbol{\Psi}_i^h & \boldsymbol{\Phi}_i^h \end{pmatrix}, \tag{12}$$

and $\mathrm{bdiag}_{h=0,\ldots,\tilde{N}}(\cdot)$ designates a block-diagonal matrix with the arguments being the h^{th} block of a matrix. Combining the transformations from Eq. (3) and Eq. (11), the physical displacement of the entire cyclic stage can be approximated by $\tilde{\mathbf{p}}(t)$, i.e.,

$$\mathbf{x}(t) \simeq (\mathbf{F}_{N,N} \otimes \mathbf{I}_{N_s})\boldsymbol{\Phi}_{\mathcal{CB}}\ \tilde{\mathbf{p}}(t), \tag{13}$$

where the size of the vector $\tilde{\mathbf{p}}(t)$ is much less than that of $\mathbf{x}(t)$. It is noted that the motion of the inter-stage boundary is now represented as

$$\mathbf{x}_b(t) = (\mathbf{F}_{N,N} \otimes \mathbf{I}_{N_b})\tilde{\mathbf{u}}_b(t). \tag{14}$$

B. Reduced Order Modeling of Non-Cyclic Stages

Let us assume that stage 2 consists of M sectors and does not possess cyclic-symmetry. Fig. 2 shows stage 2 where M equals 23. Furthermore, let us also assume that the dynamics of this stage cannot be projected onto the tuned system modes for this stage. Hence, the model may not be reduced by a method based on cyclic-symmetry as done in the previous section. In this paper, stage 2 is assumed to have a cracked blade which also induces a nonlinearity caused by the intermittent contact at the crack surfaces. Let all FE nodal displacements of stage 2 be denoted by $\mathbf{y}(t)$. The equation of motion can be written as

$$\boldsymbol{\mu}_2\ddot{\mathbf{y}}(t) + \boldsymbol{\kappa}_2\mathbf{y}(t) = \mathbf{f}(\mathbf{y}), \tag{15}$$

where $\boldsymbol{\mu}_2$ and $\boldsymbol{\kappa}_2$ denote mass and stiffness matrices, and $\mathbf{f}$ denotes a vector of nonlinear forces due to the intermittent contact at the crack surfaces. The nodal displacement vector can be partitioned as

$$\mathbf{y}(t) = \begin{bmatrix} \mathbf{y}_b(t) \\ \mathbf{y}_i(t) \end{bmatrix}, \tag{16}$$

where $\mathbf{y}_b$ contains all the displacements of the nodes on the inter-stage boundary, and $\mathbf{y}_i$ contains the rest of the internal DOFs. There are various ways to reduce the number of DOFs in the i-partition. In this paper, the motion of $\mathbf{y}$ is expressed as a linear combination of static constraint modes $\boldsymbol{\Psi}$ associated with the

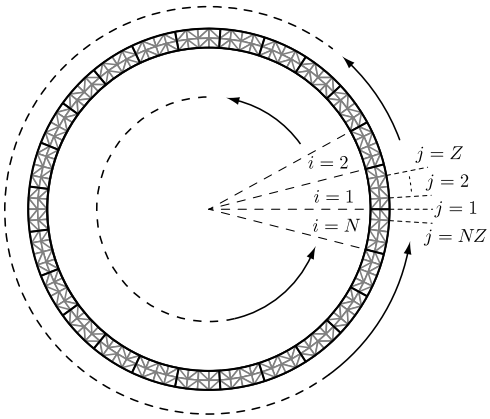

Figure 3. Inter-stage boundary (b-partition) for a cyclic stage (i denotes a sector, j denotes a radial line segment).

inter-stage boundary, and a set of modified free-interface normal modes $\hat{\mathbf{\Phi}}$ as was employed by Saito *et al.*[21] Namely,

$$\begin{bmatrix} \mathbf{y}_b(t) \\ \mathbf{y}_i(t) \end{bmatrix} \simeq \begin{pmatrix} \mathbf{I}_{N_{\tilde{b}}} & \mathbf{0} \\ \mathbf{\Psi}_i & \hat{\mathbf{\Phi}}_i \end{pmatrix} \begin{bmatrix} \mathbf{y}_b(t) \\ \mathbf{q}(t) \end{bmatrix}, \tag{17}$$

where $N_{\tilde{b}}$ is the number of DOF along the inter-stage boundary for stage 2, $\hat{\mathbf{\Phi}}_i = \mathbf{\Phi}_{ii} - \mathbf{\Psi}_i \mathbf{\Phi}_{ib}$, with $\mathbf{\Phi}_{ii}$ and $\mathbf{\Phi}_{ib}$ denoting the interior and the inter-stage boundary partitions of $\mathbf{\Phi}$ respectively. Herting[24] provides a detailed formulation of this type of CMS.

C. Inter-Stage Coupling

After constructing the ROMs of all cyclic and all non-cyclic stages, the next step is to assemble the stages, which means that the geometric compatibility conditions should be applied to the inter-stage boundary nodes. However, the FE meshes of all stages do not necessarily match at the inter-stage interfaces. Most importantly, the stages do not necessarily have the same number of sectors, which means that the stages do not possess the same periodicity. In this paper, the method proposed by Song *et al.*[4] is extended for the case with coupling between cyclic and non-cyclic stages. Namely, the motion of the inter-stage nodes are projected onto harmonic functions that are periodic in the circumferential direction. For the cyclic stage, let us first partition the displacement vector for the inter-stage boundary DOF as follows

$$\mathbf{x}_b = \begin{bmatrix} \mathbf{x}_{b_1} \\ \vdots \\ \mathbf{x}_{b_N} \end{bmatrix}, \tag{18}$$

where $\mathbf{x}_{b_i}$ corresponds to the inter-stage boundary partition of the nodal displacements of the i^{th} sector. We also assume that the FE nodes of the inter-stage boundary of each sector are aligned such that the nodes can be divided into another kind of groups of nodes having the same angle in a cylindrical coordinate system. The number of such groups in each sector is denoted here as Z, and each group is referred to as a radial line segment in this paper. This means that the inter-stage boundary of stage 1 consists of NZ radial line segments. Each radial line segment for stage 1 is considered to have N_r DOF, and each radial line segment for stage 2 is considered to have M_r DOF. The schematic depicting the inter-stage boundary and the radial line segments is illustrated in Fig. 3. Namely, $\mathbf{x}_b$ can also be partitioned as

$$\mathbf{x}_b = \begin{bmatrix} \mathbf{x}_{r_1} \\ \vdots \\ \mathbf{x}_{r_{NZ}}, \end{bmatrix} \tag{19}$$

where the subscript r stands for the radial line segment. Note that there is a relationship between $\mathbf{x}_{b_i}$ and $\mathbf{x}_{r_j}$ such that $\mathbf{x}_{b_i}$ contains $\mathbf{x}_{r_j}$ for $1+(i-1)Z \leqslant j \leqslant iZ$.

Next, we assume that the motion of the j^{th} radial segment can be *approximated* by a truncated Fourier series. Namely, defining $\theta_h \triangleq 2\pi h/(NZ)$,

$$\mathbf{x}_{r_j} \simeq \frac{1}{\sqrt{B}}\mathbf{z}^0 + \sqrt{\frac{2}{B}}\sum_{h=1}^{P-1}\left(\mathbf{z}_c^h \cos(j-1)\theta_h + \mathbf{z}_s^h \sin(j-1)\theta_h\right) + \frac{1}{\sqrt{B}}(-1)^{j-1}\mathbf{z}^P, \tag{20}$$

where $\mathbf{z}$ represents the Fourier coefficients with superscript denoting the harmonic number and subscript denoting either cosine or sine term, and B is the number of basis harmonic functions used for the Fourier expansion. Note that $P = B/2$ if B is even. If B is odd, $P = (B-1)/2$ and the last term in Eq. (20) does not exist. Therefore, in matrix form,

$$\mathbf{x}_b = \begin{bmatrix} \mathbf{x}_{r_1} \\ \vdots \\ \mathbf{x}_{r_{NZ}} \end{bmatrix} \simeq \left(\mathbf{F}_{NZ,B} \otimes \mathbf{I}_{N_r}\right)\tilde{\mathbf{z}}, \tag{21}$$

where recall that N_r is the number of DOF per radial line segment for stage 1, $\mathbf{F}_{NZ,B}$ is a $NZ \times B$ Fourier matrix, and $\tilde{\mathbf{z}} = [(\mathbf{z}^0)^{\mathrm{T}}, (\mathbf{z}_c^h)^{\mathrm{T}}, (\mathbf{z}_s^h)^{\mathrm{T}}, \ldots, (\mathbf{z}^P)^{\mathrm{T}}]^{\mathrm{T}}$. Inverting Eq. (14) and combining it with Eq. (21),

$$\tilde{\mathbf{u}}_b(t) \simeq \left(\mathbf{F}_{N,N} \otimes \mathbf{I}_{N_b}\right)^{\mathrm{T}}\left(\mathbf{F}_{NZ,B} \otimes \mathbf{I}_{N_r}\right)\tilde{\mathbf{z}}. \tag{22}$$

For the non-cyclic stage (stage 2), the displacement vector of the inter-stage boundary $\mathbf{y}_b$ can be partitioned as

$$\mathbf{y}_b = \begin{bmatrix} \mathbf{y}_{b_1} \\ \vdots \\ \mathbf{y}_{b_M} \end{bmatrix}. \tag{23}$$

Furthermore, as was done for the cyclic stage (stage 1), $\mathbf{y}_{b_i}$ can also be partitioned based on the radial line segments, i.e.,

$$\mathbf{y}_{b_i} = \begin{bmatrix} \mathbf{y}_{r_1} \\ \vdots \\ \mathbf{y}_{r_W} \end{bmatrix}, \tag{24}$$

where W is the number of radial line segments per sector. Next, the motion of the inter-stage boundary is represented by a truncated Fourier series assuming that the number of basis harmonic functions is the same as the one used for the cyclic stage. Namely,

$$\mathbf{y}_b = \begin{bmatrix} \mathbf{y}_{r_1} \\ \vdots \\ \mathbf{y}_{r_{MW}} \end{bmatrix} \simeq \left(\mathbf{F}_{MW,B} \otimes \mathbf{I}_{M_r}\right)\tilde{\mathbf{w}}, \tag{25}$$

where $\tilde{\mathbf{w}}$ is a vector of Fourier coefficients, i.e., $\tilde{\mathbf{w}} = [(\mathbf{w}^0)^{\mathrm{T}}, (\mathbf{w}_c^h)^{\mathrm{T}}, (\mathbf{w}_s^h)^{\mathrm{T}}, \ldots, (\mathbf{w}^P)^{\mathrm{T}}]^{\mathrm{T}}$. Recall that M_r is the number of DOF per radial line segment for stage 2. In this paper, it is assumed that $N_r = M_r$.

At this point, the displacement of the inter-stage boundary of the cyclic and non-cyclic stages are represented by vectors of Fourier coefficients $\tilde{\mathbf{z}}$ and $\tilde{\mathbf{w}}$. The geometric compatibility condition is now enforced as

$$\tilde{\mathbf{z}} = \tilde{\mathbf{w}}. \tag{26}$$

Even though the compatibility conditions are enforced approximately, as long as a sufficient number of Fourier coefficients B are used, the geometric compatibility conditions are very well imposed.[1]

IV. Analysis

Two ROMs were developed using the methodology presented in the *Mathematical Formulation* section and are numerically validated in this section. Both ROMs were developed only from FEMs of single stage

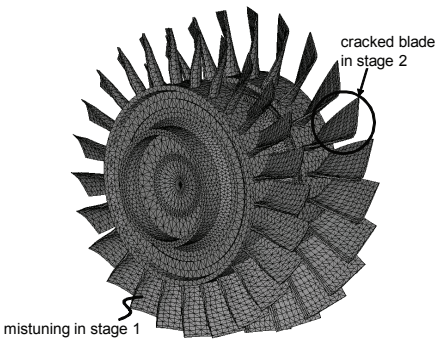

Figure 4. FEM of multi-stage turbomachinery rotor.

models created in ANSYS. To validate the ROMs, two full-order multi-stage FEMs were also created in ANSYS. These two multi-stage systems differ only in stage 2. A full-order multi-stage FEM of one of the two multi-stage systems is shown in Fig. 4.

Stage 1 of both full-order multi-stage FEMs has 25 identical blades and 63,996 DOFs. Stage 1 also has blade-to-blade small mistuning (in the blade stiffness) with standard deviation of 0.04%. Stage 2 of one of the full-order multi-stage FEM has 23 identical blades and 74,886 DOFs. Stage 2 of the other full-order multi-stage FEM has 23 identical blades (one of which has a cracked blade), and has 76,404 DOFs. The crack occurs at the leading edge of one of the blades and has a length of about one third of the chord.

To create the multi-stage FEMs, multi-point constraint equations were applied at the inter-stage boundaries to connect the individual stages in ANSYS. The total number of DOFs for the FEM of the multi-stage system with a crack is 138,006. The corresponding ROM for the system with a crack contains 705 DOFs (0.5% of the original FE size). The total number of DOFs for the multi-stage system without a crack is 136,488. The corresponding ROM for the system without a crack is 592 DOFs (0.4% of the original FE size). Each ROM uses 23 basis functions to model the dynamics at the interface between stages (as discussed in the *Inter-Stage Coupling* section).

The ROMs were developed to be valid over a frequency range of $0-20$ kHz. The bulk of the results below are focused on a narrower frequency range of $0-5$ kHz, where multi-stage modes and crack effects interact. In this work, multi-stage modes refer to modes that are not dominated by motion in a single stage, rather both stages respond at these frequencies. Note that the effects which multi-stage phenomena have on the dynamics in the presence of cracks are of particular interest since this topic has not yet been explored. Also, in this work nonlinear forced response results were computed for the ROMs using a hybrid frequency/time domain method, which prevents inter-penetration at the crack surfaces using a penalty coefficient as done by Saito *et al.*[21]

Before studying the interactions between the multi-stage and crack effects the ROMs were validated with respect to the full FEMs. The relative error of the ROM frequencies with respect to their FEM for the first 200 modes was less than 0.05%. Additionally, linear forced response calculations were validated (for the ROM with a crack and the ROM without a crack) in the multi-stage frequency regime $2.8-3.4$ kHz. The error at the peak responses for both ROMs was approximately 1% on both stages. For all forced response calculations in this work, a proportional damping $\mathbf{C} = \alpha\mathbf{M} + \beta\mathbf{K}$ was applied to the system. Here, $\mathbf{C}$ is the damping matrix with $\alpha = 1.9295 \times 10^{-2}$ and $\beta = 5.1340 \times 10^{-5}$. Engine order 1 excitation was applied to nodes at the blade tips of each stage. Since the multi-stage modes were of particular interest, forced responses were calculated at 1,024 evenly sampled frequencies from 2.8 kHz to 3.4 kHz.

Figure 5 displays the multi-stage forced response results for three different cases. The first case is a forced response analysis for the ROM of the system without a crack. The second case corresponds to a forced response analysis using a ROM of a system with a crack and a linear analysis (allowing inter-penetration). The final case corresponds to a forced response using a ROM of a system with a crack and a nonlinear analysis (not allowing inter-penetration at the crack surfaces as done by Saito *et al.*[21]). The results for stage 1 are shown in Fig. 5(a) and the results for stage 2 are shown in Fig. 5(b).

The differences between the responses for stage 1 are not nearly as large as the differences for stage 2, since the crack is located in stage 2. For stage 1, the largest response for the peak near 3.2 kHz is predicted

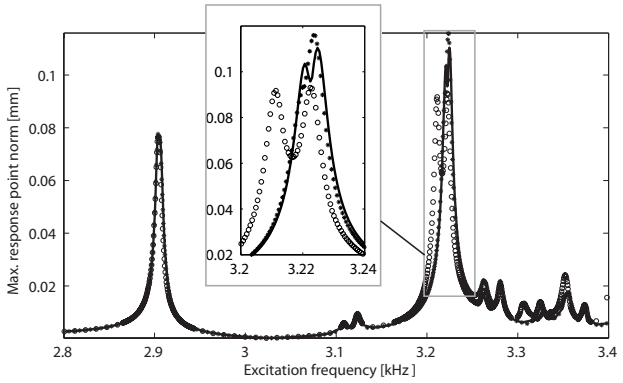

(a)

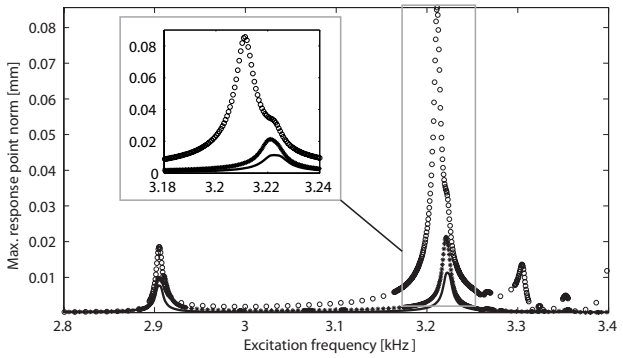

(b)

Figure 5. Comparison of the multi-stage forced response for the ROM of the system without a crack (-), for the ROM of the system with a crack using a linear analysis (o), and for a ROM of the system with a crack using a nonlinear analysis (*) for (a) stage 1 and (b) stage 2.

by the nonlinear forced response analysis. This response is only about 5% larger than the response of the system without a crack and 25% larger than the linear forced response.

For stage 2, the structural response is as expected for all three cases. The system without a crack is the stiffest and has the lowest amplitude. The linear forced response for the system with a crack is the softest and has the largest amplitude. In fact, the peak response near 3.2 kHz is almost eight times that of the system without a crack. The nonlinear forced response amplitude for the system with a crack is between the other two cases. However, the range of amplitudes between the two cases is very large. Hence, performing the nonlinear analysis is very important in obtaining an accurate response for the stage with a crack. For the peak response near 3.2 kHz, the nonlinear analysis yields a response of just 25% of that obtained using a linear analysis, but double that of the system with no crack.

A plot of the mode shape corresponding to the natural frequency at 3.21 kHz for the FEM of the multi-stage system with a crack is shown in Fig. 6 to better understand the results in Fig. 5. Fig. 6 shows that the motion in stage 1 is distributed throughout the stage, which explains why the response of stage 1 is not greatly affected by the crack in stage 2. In contrast, the motion of stage 2 is localized to the cracked blade; therefore a full nonlinear analysis is critical in accurately capturing the response of the cracked blade.

To show the importance of the multi-stage modeling, a single-stage analysis was conducted on stage 2 (with both of its inter-stage surfaces being fixed). The results are summarized in Fig. 7. The forced response was computed for $4,092$ evenly spaced frequencies in the range $1.5 - 4.5$ kHz. This larger range was chosen since the response is very low. That is because the modes in the range $2.8 - 3.4$ kHz are multi-stage modes and are not present when a single-stage analysis is performed. The low level response in the range $2.8 - 3.4$ kHz demonstrates the need for multi-stage modeling for accurately capturing the dynamics. Three cases are plotted (nonlinear forced response of the stage with a crack, linear forced response of the stage with a crack, and the response of the same stage when it does not have a crack). The behavior is similar to

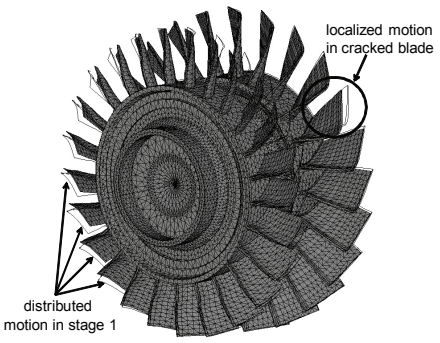

Figure 6. Mode shape corresponding to a frequency of approximately 3.21 kHz from the FEM of the multi-stage system with a crack.

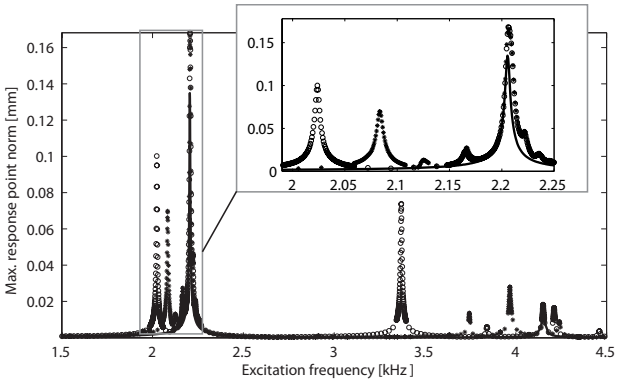

Figure 7. Comparison of the forced response for stage 2 only for the ROM of a stage that does not have a crack (-), for the ROM of the stage with a crack using a linear analysis (o), and for a ROM of the same stage with a crack using a nonlinear analysis (*).

the results in Fig. 5 in that the nonlinear forced response is bounded by the linear forced response and the response of the system without a crack.

A single-stage analysis was also conducted on stage 1 to show the importance of multi-stage modeling. The results are summarized in Fig. 8. Three cases are plotted. The first corresponds to the response of just stage 1 (with both of its inter-stage surfaces being fixed). The next two cases correspond to the response of stage 1 when a full multi-stage analysis is conducted. One of these latter two cases corresponds to the system where there is no crack in stage 2, and the other when there is a crack in stage 2 (and a nonlinear analysis is conducted). It is evident that for stage 1 the effect of single versus multi-stage modeling is very important. However, the effect of modeling the crack (in stage 2) is not that important for stage 1 (although it is important for predicting the response of stage 2).

V. Conclusions

A novel modeling methodology for combining single stage models (of different types) was introduced. The methodology was used to create reduced order models (ROMs) that combine a model of a single stage with a crack with a model of another single stage containing small blade-to-blade mistuning. The full order model of the stage with a crack was reduced using component mode synthesis (CMS), while the mistuned stage was reduced using cyclic-symmetry analysis, CMS, and component mode mistuning (CMM). The novel methodology enabled combining these two single stage ROMs with different modeling frameworks. The two stages were assembled by projecting the motion at the interface of the neighboring stages along a set of harmonic basis functions.

The results presented demonstrate the interaction between multi-stage effects and cracked-blade effects

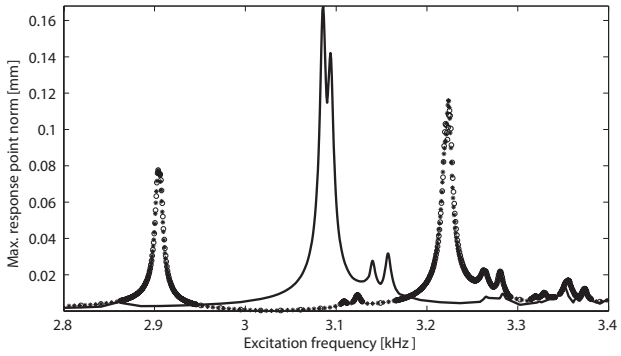

Figure 8. Effect of multi-stage versus stage-wise only analysis. Stage 1 only forced response (-), multi-stage results for a system without a crack (o), and nonlinear forced response for the multi-stage system with a crack (*).

on the response of the overall system. It was demonstrated that performing a multi-stage analysis (as opposed to one single-stage analysis for each individual stage) is very important in certain frequency ranges for realistic industrial blades. It was also shown that, although the nonlinear forced response of a system with a cracked blade is bounded by the linear forced response of the system with a cracked blade and the response of a system without a cracked blade, this range can be very large and only through a nonlinear analysis can the true response be predicted.

Acknowledgment

The partial financial support of the Air Force Office of Scientific Research through grant FA9550-08-1-0276 (Dr. Douglas Smith, Program Manager) is gratefully acknowledged.

References

[1]Song, S. H., *Vibration Analysis and System Identification of Mistuned Multistage Turbine Engine Rotors*, Ph.D. thesis, The University of Michigan, 2007.

[2]Castanier, M. P. and Pierre, C., "Modeling and Analysis of Mistuned Bladed Disk Vibration: Status and Emerging Directions," *Journal of Propulsion and Power*, Vol. 22, March 2006, pp. 384–396.

[3]Bladh, R., Castanier, M. P., and Pierre, C., "Effects of Multistage Coupling and Disk Flexibility on Mistuned Bladed Disk Dynamics," *Journal of Engineering for Gas Turbines and Power - Transactions of the ASME*, Vol. 125, No. 1, 2003, pp. 121–130.

[4]Song, S. H., Castanier, M. P., and Pierre, C., "Multi-Stage Modeling of Turbine Engine Rotor Vibration," *Proceedings of the ASME 2005 Design Engineering Technical Conference and Computers and Information in Engineering Conference*, Long Beach, CA, USA, September 2005, DETC2005-85740.

[5]Song, S. H., Castanier, M. P., and Pierre, C., "Multi-Stage Modeling of Mistuned Turbine Engine Rotor Vibration," *Proceedings of the NATO AVT-121 Symposium on Evaluation, Control and Prevention of High Cycle Fatigue in Gas Turbine Engines for Land, Sea, and Air*, Granada, Spain, October 2005, RTO-MP-AVT-121-P-06.

[6]Lim, S.-H., Bladh, R., Castanier, M. P., and Pierre, C., "Compact, Generalized Component Mode Mistuning Representation for Modeling Bladed Disk Vibration," *AIAA Journal*, Vol. 45, No. 9, 2007, pp. 2285–2298.

[7]Song, S. H., Castanier, M. P., and Pierre, C., "System Identification of Multistage Turbine Engine Rotors," *Proceedings of GT2007 ASME Turbo Expo*, Montreal, Canada, May 2007, GT2007-28307.

[8]Laxalde, D., Thouverez, F., and Lombard, J.-P., "Dynamical Analysis of Multi-Stage Cyclic Structures," *Mechanics Research Communications*, Vol. 34, No. 4, 2007, pp. 379–384.

[9]Laxalde, D., Lombard, J.-P., and Thouverez, F., "Dynamics of Multistage Bladed Disks Systems," *Journal of Engineering for Gas Turbines and Power*, Vol. 129, No. 4, 2007, pp. 1058–1064.

[10]Sternchüss, A., Balmès, E., Jean, P., and Lombard, J.-P., "Reduction of Multistage Disk Models: Application to an Industrial Rotor," *Journal of Engineering for Gas Turbines and Power*, Vol. 131, No. 1, 2009, pp. 012502.

[11]Sinha, A., "Reduced-Order Model of a Mistuned Multi-Stage Bladed Rotor," *International Journal of Turbo and Jet Engines*, Vol. 25, No. 3, 2008, pp. 145–153.

[12]Chatelet, E., D'Ambrosio, F., and Jacquet-Richardet, G., "Toward Global Modeling Approaches for Dynamic Analyses of Rotating Assemblies of Turbomachines," *Journal of Sound and Vibration*, Vol. 282, No. 1-2, 2005, pp. 163–178.

[13]Turhan, O. and Bulut, G., "Linearly Coupled Shaft-Torsional and Blade-Bending Vibrations in Multi-Stage Rotor-Blade Systems," *Journal of Sound and Vibration*, Vol. 296, No. 1-2, 2006, pp. 292–318.

[14]Rzadkowski, R. and Sokolowski, J., "Coupling Effects Between the Shaft and Two Bladed-Discs," *Advances in Vibration Engineering*, Vol. 4, No. 3, 2005, pp. 249–266.

[15]Rzadkowski, R. and Drewczynski, M., "Coupling of Vibration of Several Bladed Discs on the Shaft, Part I: Free Vibration Analysis," *Advances in Vibration Engineering*, Vol. 8, No. 2, 2009, pp. 125–137.

[16]Seguì, B. and Casanova, E., "Application of a Reduced Order Modeling Technique for Mistuned Bladed Disk-Shaft Assemblies," *Proceedings of GT2007 ASME Turbo Expo*, May 2007, GT2007-27594.

[17]Craig, R. R. and Bampton, M. C. C., "Coupling of Substructures for Dynamic Analyses," *AIAA Journal*, Vol. 6, No. 7, 1968, pp. 1313–1319.

[18]Boulton, L. A. and Casanova, E., "Reduced Order Model for a Two Stage Gas Turbine including Mistuned Bladed Disks and Shaft Interaction," *Proceedings of the GT2009 ASME Turbo Expo*, Jun 2009, GT2009-59335.

[19]Laxalde, D. and Thouverez, F., "Non-Linear Vibrations of Multi-Stage Bladed Disks Systems with Friction Ring Dampers," *Proceedings of the ASME International Design Engineering Technical Conferences and Computers and Information in Engineering Conference 2007, Paper DETC2007-34473*, ASME, Las Vegas, Nevada, USA, September 2007.

[20]Nacivet, S., Pierre, C., Thouverez, F., and Jezequel, L., "A Dynamic Lagrangian Frequency-Time Method for the Vibration of Dry-Friction-Damped Systems," *Journal of Sound and Vibration*, Vol. 265, No. 1, Jul 2003, pp. 201–219.

[21]Saito, A., Castanier, M. P., and Pierre, C., "Effects of a Cracked Blade on Mistuned Turbine Engine Rotor Vibration," *Journal of Vibration and Acoustics - Transactions of the ASME*, Vol. 131, No. 6, 2009, pp. 061006.

[22]Kharyton, V., Laine, J.-P., Thouverez, F., and Kucher, O., "Cracked Blade Detection from Bladed Disk Forced Response," *Proceedings of the GT2009 ASME Turbo Expo*, 2009, GT2009-59598.

[23]Bladh, R., Castanier, M. P., and Pierre, C., "Component-Mode-Based Reduced Order Modeling Techniques for Mistuned Bladed Disks - Part I: Theoretical Models," *Journal of Engineering for Gas Turbines and Power - Transactions of the ASME*, Vol. 123, No. 1, 2001, pp. 89–99.

[24]Herting, D. N., "A General Purpose, Multi-Stage, Component Modal Synthesis Method," *Finite Elements in Analysis and Design*, Vol. 1, No. 2, 1985, pp. 153–164.